Research Square

Preprints are preliminary reports that have not undergone peer review.
They should not be considered conclusive, used to inform clinical practice,
or referenced by the media as validated information.

Tight drill-stem tests as in-situ matrix permeability tests: how much of the gas in a fractured quartzite can be produced? Attahaddy Field, Sirte Basin, Libya

Gheith Alfakri

Ghate_emg@yahoo.com

Sirte Oil Company

Research Article

Keywords: drill-stem test, tight gas, matrix permeability, naturally fractured reservoir, pressure derivative, recovery factor, quartzite, legacy data, Sirte Basin

Posted Date: November 12th, 2026

DOI: https://doi.org/10.21203/rs.3.rs-11510669/v1

License: This work is licensed under a Creative Commons Attribution 4.0 International License.
Read Full License

Additional Declarations: No competing interests reported.

Tight drill-stem tests as in-situ matrix permeability tests: how much of the gas in a fractured quartzite can be produced? Attahaddy Field, Sirte Basin, Libya

Dr .Gheith Alfakri

Exploration Department, Sirte Oil Company, Marsa El Brega, Libya

Corresponding author: Ghate_emg@yahoo.com

Abstract

In tight fractured gas reservoirs most of the gas is stored in the matrix, but the matrix permeability that controls whether this gas reaches the fractures is often below what routine core analysis can measure. In the Cambro-Ordovician Gargaf quartzite of the Attahaddy Field, Sirte Basin, Libya, 37 of 44 core plugs read zero permeability (below about 0.05 mD), so whether the gas in place can be produced has been unknown. We show that drill-stem tests (DSTs) that flowed little or nothing, usually dismissed as failures, help to answer this, because they test the rock between conductive fractures in situ. Pressure–time records of nine DSTs in seven wells (1987–1997) were recovered from scanned well files by optical character recognition and transcription, and analysed with gas pseudo-pressure and Bourdet derivatives. Gas tests flowing 5.5–11.7 MMcf/d give interval-average permeabilities of 0.26–4.5 mD (two of them lower bounds), and a weak test at least 0.11 mD, after an early derivative hump caused by wellbore storage and positive skin. The tight Gargaf test FF12 DST-2, which produced no fluid to surface, gives a lower bound of 1.6–2.6 μD; together with the core detection limit this brackets the permeability of the rock between flowing fractures at about 2–50 μD. A low-permeability test (FF21 DST-2, 5.5 μD) proves to overlap the productive zone of an earlier test in the same well, showing that low DST permeability can also reflect damage. A real-gas diffusion model of matrix blocks bounded by fractures, with block sizes from the conductive-fracture spacing inferred from 60 Gargaf DSTs (mean 383 ft; 218 ft and 559 ft in areas of bright and dim top-reservoir seismic amplitude), shows that even at the 2-μD lower bound about 90% of the matrix gas drains to the fractures within 30 years; the drained fraction would fall to 80% only below about 0.6 μD and to 50% below about 0.07 μD. With gas initially in place of 5.3 Tcf (P10–P90 3.7–7.4), 4.0 Tcf (2.8–5.7) is technically drainable to a 1,000 psia abandonment pressure for the bracketed permeability. Mapped with the 3D seismic, the main difference between bright and dim areas lies in reaching the fractures: an open interval needs about 500 ft to have a 90% chance of meeting a flowing fracture where the top reflection is bright, and about 1,300 ft where it is dim. Recovery in this field is therefore limited by how much of the fracture network is connected to wells, and by water entering through the fractures, rather than by the tightness of the matrix.

Keywords: drill-stem test; tight gas; matrix permeability; naturally fractured reservoir; pressure derivative; recovery factor; quartzite; legacy data; Sirte Basin

Highlights

- Pressure data from nine legacy drill-stem tests were recovered from scanned well files
- A tight test bounds the permeability between flowing fractures at no less than about 2 μD
- With the core limit, the matrix is bracketed at about 2–50 μD

- Even at 2 μD about 90% of the matrix gas drains to fractures in 30 years
- Seismic maps show where wells need longer intervals to meet a flowing fracture
- Recovery is limited by fracture connectivity and water, not by the tight matrix

1. Introduction

In naturally fractured reservoirs the fractures carry the flow and the matrix holds most of the fluid [1–3]. How much of the stored fluid can be produced depends on how fast it moves from the matrix into the fractures, which is controlled by the matrix permeability and by the size of the matrix blocks between conductive fractures [1, 4]. In tight gas reservoirs both quantities are hard to measure. Matrix permeability is often below the resolution of routine core analysis, and the spacing of the fractures that actually conduct cannot be read from cores or image logs, which record many closed or healed fractures [2, 5].

The Gargaf quartzite of the Attahaddy gas field, Sirte Basin, Libya [6, 7], is an extreme example. Average matrix porosity is about 3%, and 37 of 44 core plugs read zero permeability: the matrix is tighter than about 0.05 mD, but by how much is unknown. Gas flows from a small number of conductive fractures, whose mean spacing along the hole has been estimated at about 340–380 ft from the outcomes of Gargaf DSTs [8, 9]. Two opposite conclusions are possible. If the matrix is permeable enough, the gas in it drains to the fractures and most of the gas in place is recoverable. If it is too tight, only the gas near fractures is produced and much of the gas in place is stranded.

Drill-stem tests offer a way to decide. A DST measures the permeability of the rock around the well over a radius of feet to hundreds of feet [10, 11]. Tests that flowed strongly measure the fracture system. Tests that flowed weakly or not at all are usually recorded as failures, yet they measure the rock between conductive fractures in situ, the quantity that core could not resolve. At Attahaddy, the pressure records of these tests survive only as printed tables and charts in scanned well files. This paper recovers them and asks:

1. What is the in-situ permeability of the Gargaf between conductive fractures, as constrained by tight and low-rate DSTs, and how does it compare with the fracture system measured by gas tests?
2. At that permeability, and with matrix blocks of the size implied by the conductive-fracture spacing, how much of the matrix gas drains to the fractures within a field life?
3. How much of the gas in place is therefore recoverable, and what limits it?

2. Geological setting and data

The Attahaddy Field lies at the northern end of the Zelten Platform in the central Sirte Basin [6, 7]. The trap is a NW–SE faulted anticline about 25 km long. The Gargaf Formation is a hard, brittle orthoquartzite cemented by syntaxial quartz overgrowths [12], overlain unconformably by Upper Cretaceous sandstones and shales of the Bahi and Maragh formations or, on the crest, by the Kalash limestone [13, 14]. Build-ups reach 5,350–5,620 psia at gauge depths of 9,700–12,300 ft, temperatures are about 290–320 °F, and the gas is lean (about 90% methane, gas gravity about 0.68, from DST samples). Companion studies place the water level at about −12,117 ft subsea [15] and show that formation water reaches the wells through fractures that logs and cores do not detect [8].

Well files of seven wells contained DST pressure data in a usable form (Table 1, Fig. 1). The 1987 tests of FF12 are typed Halliburton breakdown sheets, listing pressure against time minute by minute. The 1993 tests of FF21 are computer listings of mechanical gauges. The 1996–1997 tests of FF29–FF33 are listings of electronic quartz gauges recorded every 8 s to 15 min. Seven tests are in the Gargaf; FF33 DST-2 and FF21 DST-1 include 17–25 ft above the Gargaf top, FF29 DST-1 92 ft, FF32 DST-2 about 200 ft and FF31 DST-1 about 315 ft of the overlying Bahi or Maragh. FF12 DST-1 lies entirely above the Gargaf top (12,233 ft). FF30 DST-1 begins 43 ft below the Maragh top in a well where the Gargaf top was not reported, and the test report describes the interval as volcanics and Bahi; both tests are reported for comparison only. The core data are routine plug porosity and air permeability from 11 Gargaf wells [8].

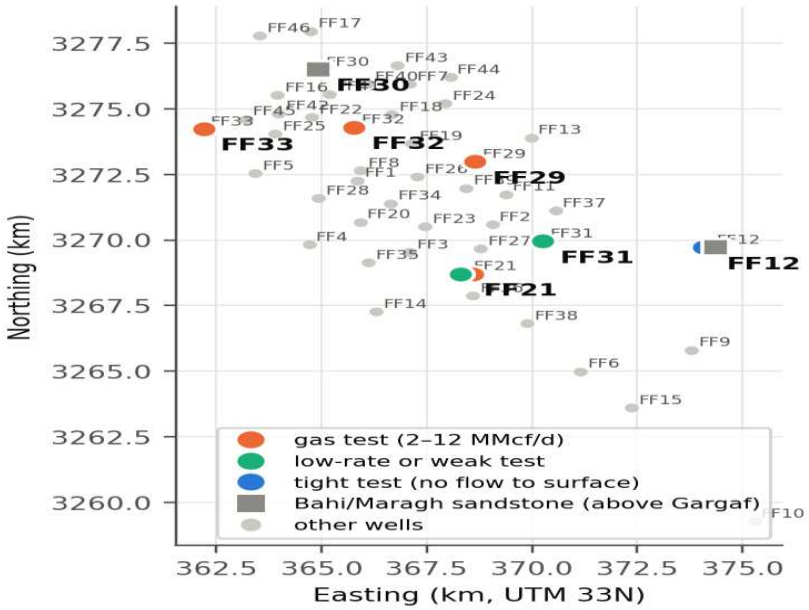


Fig. 1. Location of the wells whose DSTs were analysed, coloured by test outcome, among the other Attahaddy wells. Wells FF21 and FF12 each have two tests; the symbols are offset slightly.

Table 1. The nine DSTs analysed. Interval: open hole tested (ft, measured depth). Flow: total flow time before the final build-up; build-up: duration of the final build-up analysed. Rate: surface gas rate during the final flow as estimated at the well site from wellhead pressure on a ½-inch choke (* estimated in this study from the same relation; see Section 3.2).

Test	Year, data	Interval (ft)	Formation	Flow / build-up (h)	Rate (MMcf/d)	Outcome
FF33 DST-2	1997, electronic	11,149–11,677	Gargaf	5.2 / 13.9	11.7	gas
FF21 DST-1	1993, mechanical	9,734–9,988	Gargaf	1.0 / 2.5	8	gas
FF29 DST-1	1996, electronic	10,836–11,368	Gargaf (92 ft Bahi above)	7.2 / 13.8	5.5	gas
FF32 DST-2	1997, electronic	9,868–11,176	Gargaf + Bahi	7.2 / 13.2	≈8.4*	gas
FF21 DST-2	1993, mechanical	9,750–10,533	Gargaf (overlaps DST-1)	24.1 / 43.7	2	gas, low rate
FF31 DST-1	1997, electronic	10,473–11,237	Gargaf + Bahi/Maragh	8.2 / 16.2	≈1*, with water	weak gas + formation water
FF12 DST-2	1987, typed sheet	12,331–12,607	Gargaf	1.0 / 2.0	0	tight: no fluid to surface

Test	Year, data	Interval (ft)	Formation	Flow / build-up (h)	Rate (MMcf/d)	Outcome
FF30 DST-1	1997, electronic	10,877–11,091	Maragh/Bahi or volcanics (uncertain)	7.6 / 14.6	0.03–0.3*	weak gas, wellhead pressure fell to zero
FF12 DST-1	1987, typed sheet	11,886–12,204	Bahi/Maragh	2.3 / 2.0	trace (5 psi)	weak gas

3. Methods

3.1 Recovering the pressure records

Pages of pressure listings were rendered at 300 dpi and read with the Tesseract optical character recognition engine. Lines beginning with a clock time were parsed into time, pressure and temperature, the date was carried from the page headings, and the gauge closest to the tested interval was used. Common recognition errors (for example "§" or "$" for "5", spaces inside numbers) were corrected by rule, duplicated times were merged, and values departing by more than 6% from a seven-point running median were removed (1–14 values per test). The typed 1987 breakdown sheets, which are partly hand-filled, were transcribed manually. Flow and shut-in periods were taken from the operation logs in the same reports. Each recovered series was checked against the pressures summarised by the service company at the start and end of each period.

3.2 Gas properties, rates and permeability

Gas properties were computed for a gas gravity of 0.68, with pseudo-critical properties from Sutton [16], the z-factor from Hall and Yarborough [17] and viscosity from Lee et al. [18], at the gauge temperature of each test. Pressures were converted to real-gas pseudo-pressure m(p) [19]. For the final build-up of each test, the Bourdet derivative of Δm(p) with respect to the logarithm of Agarwal equivalent time was computed with a smoothing window of 0.15 log units [20, 21]. Where the derivative was flat (radial flow), the permeability–thickness product follows from the Horner relation [10, 22]:

$$kh = 1637\, q\, T / (2.303\, D') \approx 711\, q\, T / D',$$

where kh is in mD·ft, q is the gas rate in Mscf/d, T the temperature in °R and D′ the derivative level in psi²/cP. Where the derivative was still falling at the end of the build-up, the last level gives a lower bound on kh, because the true radial level is lower [11]. Interval-average permeability is kh divided by the open-hole length tested; because flow comes from a few fractures, it is an average over the interval, not the permeability of any one layer. Radius of investigation was estimated as 0.029 (k Δt / φ μ c_t)^0.5 ft, with porosity 0.03 and gas saturation 0.6.

The surface gas rates in the reports are well-site estimates made from wellhead pressure on a ½-inch choke, and they follow a single relation of 3.95 ± 0.11 MMcf/d per 1,000 psi of wellhead pressure (FF33: 11.7 MMcf/d at 2,990 psi; FF29: 5.5 at 1,350; FF21 DST-1: 8 at 2,100; FF21 DST-2: 2 at 500). The same relation was used to estimate the rate of FF32 DST-2 (2,130–2,175 psi: about 8.4 MMcf/d). For FF31 DST-1 (150–370 psi, gas slugging with formation water) and FF30 DST-1 (up to 375 psi falling to zero, below critical flow) the estimates are orders of magnitude only. These rates are approximate, and kh scales linearly with them. FF12 DST-2 produced no fluid to surface. Its inflow, 15–25 bbl/d of liquid (mud filtrate or water), was estimated from the rise of the liquid column during

the flow period [23], and the liquid form of the Horner relation was used, kh = 70.6 q μ B / D′, with D′ in psi, a liquid viscosity of 0.19 cP and B = 1. Liquid flowing into gas-bearing rock measures an effective rather than absolute permeability, which is consistent with treating the result as a lower bound.

3.3 Matrix drainage

To estimate how fast gas leaves the matrix, each matrix block was represented as a slab of half-thickness L bounded on both faces by conductive fractures [1, 4]. Real-gas flow in the slab was solved with an implicit finite-volume scheme (40 cells, Newton–Picard iteration) using the same gas properties at 310 °F, a matrix porosity of 0.03, gas saturation 0.6 and rock compressibility 4 × 10⁻⁶ psi⁻¹. The pressure on the fracture faces falls linearly from 5,550 psia to an abandonment pressure of 1,000 psia over 30 years. The drained fraction E(t) is the gas produced from the slab divided by the gas it would have produced if its pressure had followed the fracture pressure instantly. For a small pressure step the scheme reproduces the analytical solution for slab diffusion [24] to within 0.005 in drained fraction. E was tabulated for permeabilities of 0.001–100 μD and half-thicknesses of 5–2,000 ft.

Conductive fractures were assumed to be spaced randomly along the hole, so block thicknesses follow an exponential distribution with mean equal to the conductive-fracture spacing s [8]. The field-wide mean, fitted to the outcomes and lengths of 60 Gargaf DSTs, is 383 ft (95% interval 273–553 ft); it is 218 ft in wells where the reservoir-top seismic amplitude is bright and 559 ft where it is dim [9]. The spacing along a vertical hole was taken as the block thickness, and the drained fraction of a population of blocks is the volume-weighted average of E over this distribution. Treating blocks as slabs bounded in one direction is conservative, because blocks bounded by fractures in more than one direction drain faster.

3.4 Field-scale recovery

Gas initially in place (GIIP) was estimated by Monte Carlo sampling (4,000 draws) of gross rock volume above the water level (35–48 km³, between maps with and without the basal siltstone), net-to-gross 0.70–0.85, porosity 0.025–0.045 and water saturation 0.25–0.60, with an initial gas formation volume factor of 1/237 rcf/scf. Drainable gas is GIIP × R*d* × *E, where R*d = 0.80 is the volumetric depletion recovery from 5,550 to 1,000 psia and E the drained fraction of the matrix; fracture porosity is negligible, so all gas was treated as matrix gas. Three cases were sampled for matrix permeability, each log-uniform: the bracket from the tight DST lower bound to the core detection limit (2–50 μD); a case allowing the DST bound to be ten times too high (0.2–50 μD); and a pessimistic case (0.01–0.1 μD). Conductive-fracture spacing was sampled log-normally around 383 ft with the 95% interval above.

4. Results

4.1 Pressure histories

The recovered records reproduce the pressures reported by the service companies at the start and end of each period, and the tests fall into three groups (Fig. 2). In the strong gas tests (FF33, FF21 DST-1, FF29, FF32) the bottom-hole pressure during flow stays at 2,400–5,100 psia and recovers to within 150 psi of the final build-up pressure within about 1.5 hours of shut-in. In the weak test FF31, flowing

pressure falls to about 800–1,600 psia, but the build-up is still fast. In FF21 DST-2 and in FF30, flowing pressure falls to about 900–1,300 psia and the build-up is still rising after 14–44 hours. The tight Gargaf test FF12 DST-2 shows almost no inflow during the 60-minute flow (pressure 297–371 psia) and builds up to 5,618 psia in 2 hours.

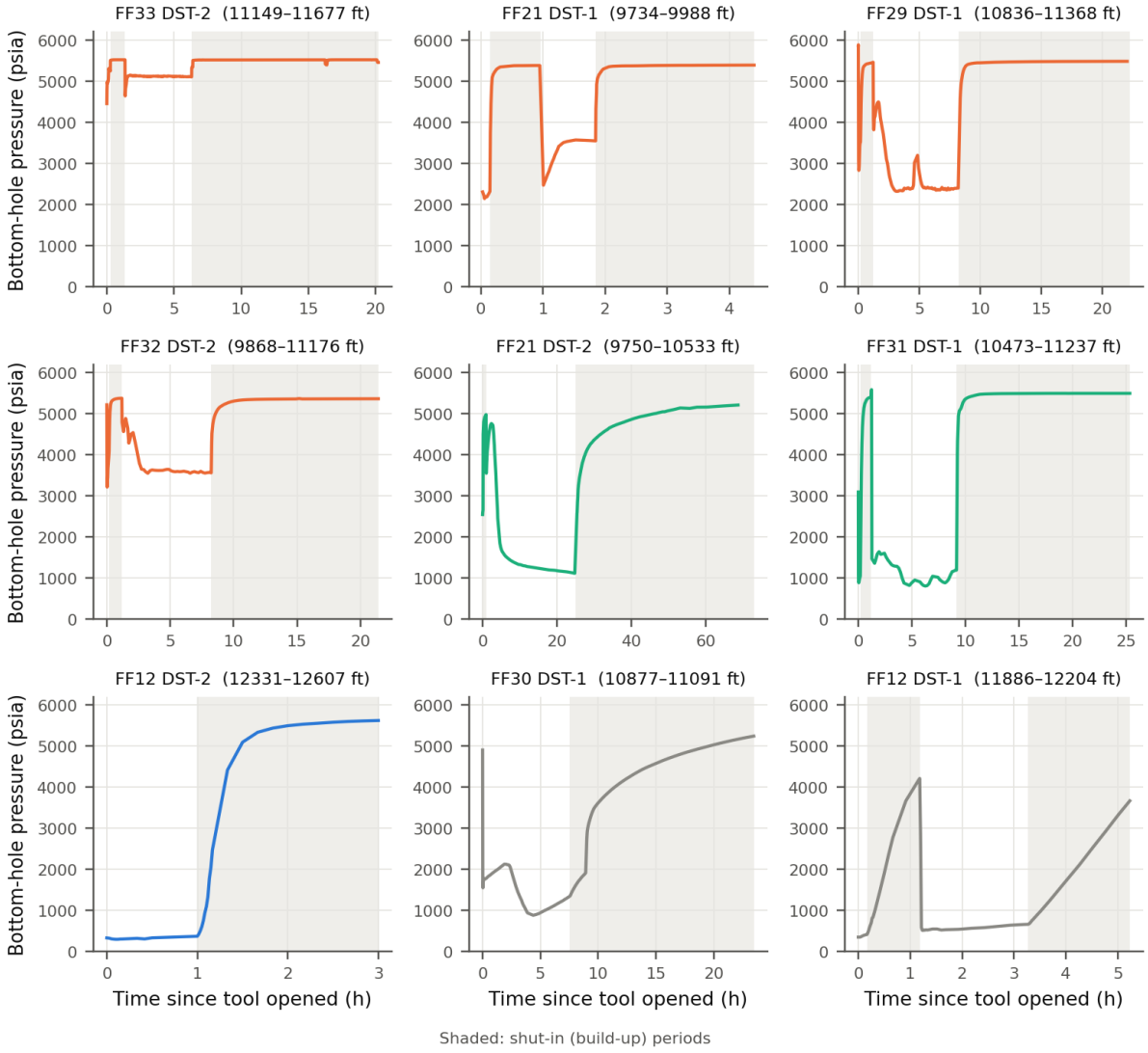


Fig. 2. Bottom-hole pressure against time for the nine DSTs, recovered from the scanned well files. Shaded: shut-in periods. Colours as in Fig. 1.

4.2 Derivative diagnostics

Most build-ups begin with a derivative hump followed by a decline (Fig. 3), the textbook signature of wellbore storage combined with positive skin [11, 20]; in DSTs, phase redistribution in the closed chamber below the tester valve can add to it. The permeability was therefore read from the level reached after the hump. In FF29 the derivative flattens at 1.5–3 hours, and in FF21 DST-2 it is flat for more than a log cycle (1–12 hours), indicating radial flow. FF33 shows a short level at 0.15–0.4 hours, but its pressure changes by less than 2% after shut-in and the derivative is noisy, so its permeability is the least precise. In FF32, FF31 and FF21 DST-1 the derivative is still falling at the end of the build-up; the last level gives lower bounds. FF12 DST-2 shows a storage hump followed by a derivative that is still falling after 2 hours, so its permeability is also a lower bound. The derivative

of FF30 rises after 1 hour, which suggests a limited connected volume. FF12 DST-1 remained dominated by wellbore storage throughout and gives no permeability.

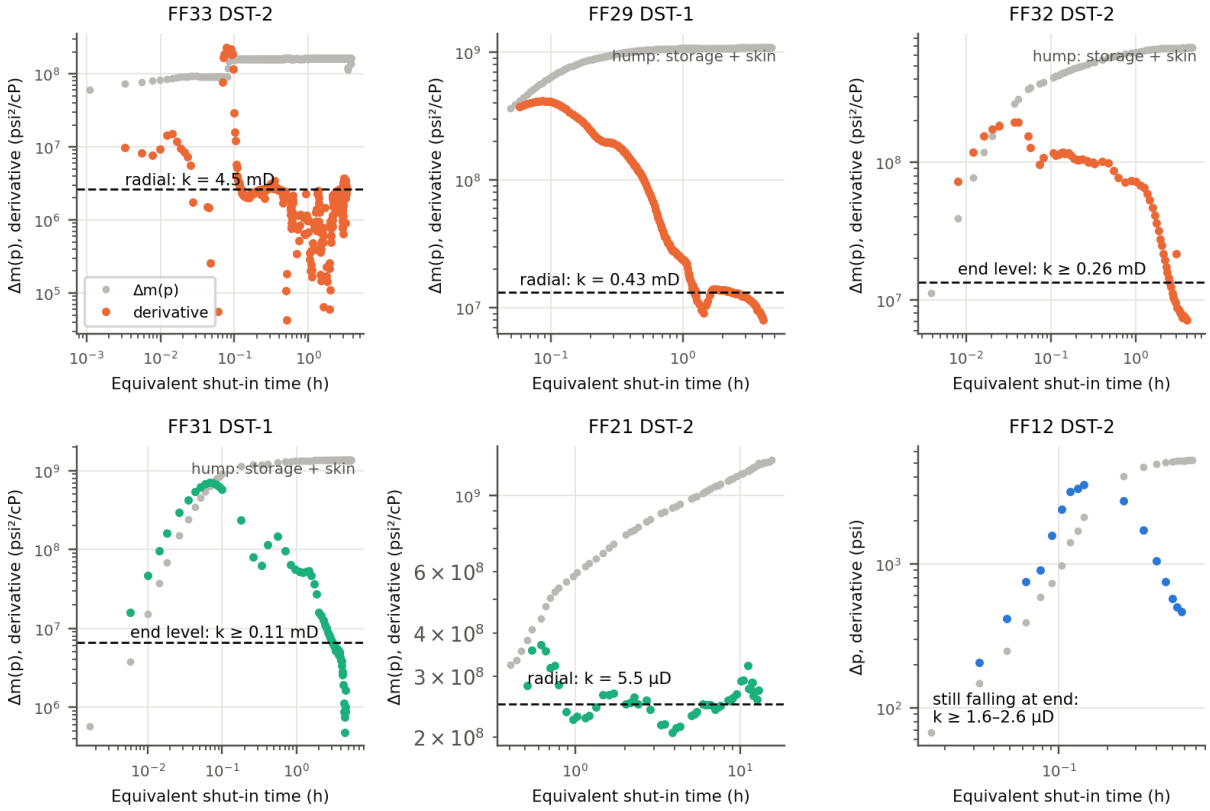


Fig. 3. Log–log diagnostic plots of the final build-ups: change in pseudo-pressure (grey) and its derivative (coloured), against Agarwal equivalent shut-in time. Dashed lines: derivative level used for permeability (radial flow, or the last level where the derivative is still falling, giving a lower bound). FF12 DST-2 is plotted in pressure (liquid inflow).

4.3 In-situ permeability

Interval-average permeability spans more than three orders of magnitude (Table 2, Fig. 4). The strong gas tests give 4.5 mD (FF33) and 0.43 mD (FF29) from radial flow, and at least 2.0 mD (FF21 DST-1) and 0.26 mD (FF32) from the last derivative level; the weak test FF31 gives at least 0.11 mD. Radii of investigation are about 55–155 ft. The early hump implies that the near-well zone of these tests is damaged or poorly connected to the fractures, so the rates measured in the DSTs understate what the same intervals could deliver.

FF21 DST-2 reached clean radial flow at only 5.5 µD (kh 4.3 mD·ft over 783 ft), although it delivered about 2 MMcf/d at a drawdown from 5,200 to 1,100 psia. Its interval (9,750–10,533 ft), however, includes 238 ft of the interval of FF21 DST-1 (9,734–9,988 ft), which a month earlier flowed 8 MMcf/d with kh of at least 510 mD·ft. The fractures that delivered DST-1 must therefore have been damaged or plugged by the time of DST-2, and its low permeability reflects damage, not the matrix. It is excluded from the matrix estimate, but it shows that a low DST permeability is a lower bound on the rock it tests.

The tight Gargaf test FF12 DST-2 gives at least 1.6–2.6 µD for an inflow of 15–25 bbl/d, within a radius of a few feet. Because damage, effective-permeability effects and a still-falling derivative can only lower the apparent value, the permeability of the rock between flowing fractures is at least about 2 µD. The core plugs place an upper limit near 50 µD, since 37 of 44 read below that value. The rock

between flowing fractures is therefore bracketed at about 2–50 µD. FF30, above or at the top of the Gargaf, gives 0.75–7.5 µD for its uncertain rate, in the same range.

Table 2. Build-up interpretation. D′: derivative level of Δm(p) (psi²/cP) in the window used. kh and k: interval-average permeability–thickness and permeability; ≥: lower bound (derivative still falling). r_inv: radius of investigation at the end of the window.

Test	q (Mscf/d)	Window (h)	D′ (psi²/cP)	kh (mD·ft)	k	Flow regime	r_inv (ft)
FF33 DST-2	11,700	0.15–0.4	2.6×10^6	2,400	4.5 mD	radial (noisy)	155
FF21 DST-1	8,000	0.3–0.55	8.4×10^6	≥510	≥2.0 mD	still falling	111
FF29 DST-1	5,500	1.5–3.0	1.3×10^7	230	0.43 mD	radial	112
FF32 DST-2	≈8,400	2.0–3.2	1.4×10^7	≥340	≥0.26 mD	still falling	96
FF31 DST-1	≈1,000	2.5–3.5	6.7×10^6	≥81	≥0.11 mD	still falling	55
FF21 DST-2	2,000	1–12	2.5×10^8	4.3	5.5 µD	radial; damaged interval	23
FF12 DST-2	15–25 bbl/d liquid	end (>1 h)	470 psi	≥0.43–0.72	≥1.6–2.6 µD	still falling	few
FF30 DST-1	30–300	0.18–0.35	1.0×10^8	0.16–1.6	0.75–7.5 µD	then limited volume	≈3
FF12 DST-1	trace	—	storage only	—	n.d.	storage	—

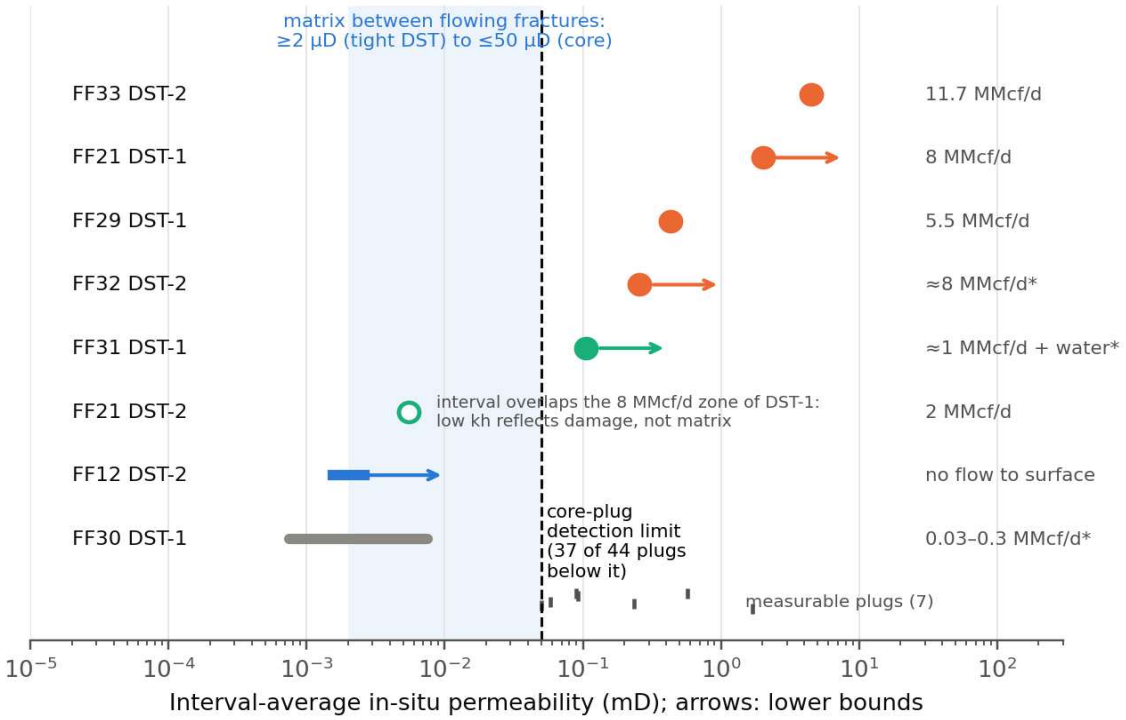


Fig. 4. Interval-average in-situ permeability from the DSTs (arrows: lower bounds; open circle: FF21 DST-2, damaged), compared with the core-plug detection limit and the seven Gargaf plugs with measurable permeability. Shaded: the bracket for the rock between flowing fractures. Rates marked * are estimated.

4.4 Matrix drainage

The drained fraction after 30 years depends on permeability and block size through the diffusion time L^2/η (Fig. 5). For a block of half-thickness 192 ft (half the mean spacing) the characteristic diffusion time at initial pressure is 0.5 years at 2 µD, 10 years at 0.1 µD and about 100 years at 0.01 µD; at 2

µD, 90% of the gas in such a block drains within about 1.7 years. Averaged over an exponential distribution of block sizes, which includes some very large blocks, the drained fraction at the 2-µD lower bound is 0.90 for the field-wide spacing of 383 ft, 0.96 where the seismic top reflection is bright (218 ft) and 0.84 where it is dim (559 ft) (Fig. 6a). For the field-wide spacing, the drained fraction falls to 0.8 at about 0.6 µD and to 0.5 at about 0.07 µD (0.02 µD in bright and 0.15 µD in dim areas), that is, 3–30 times below the lower bound.

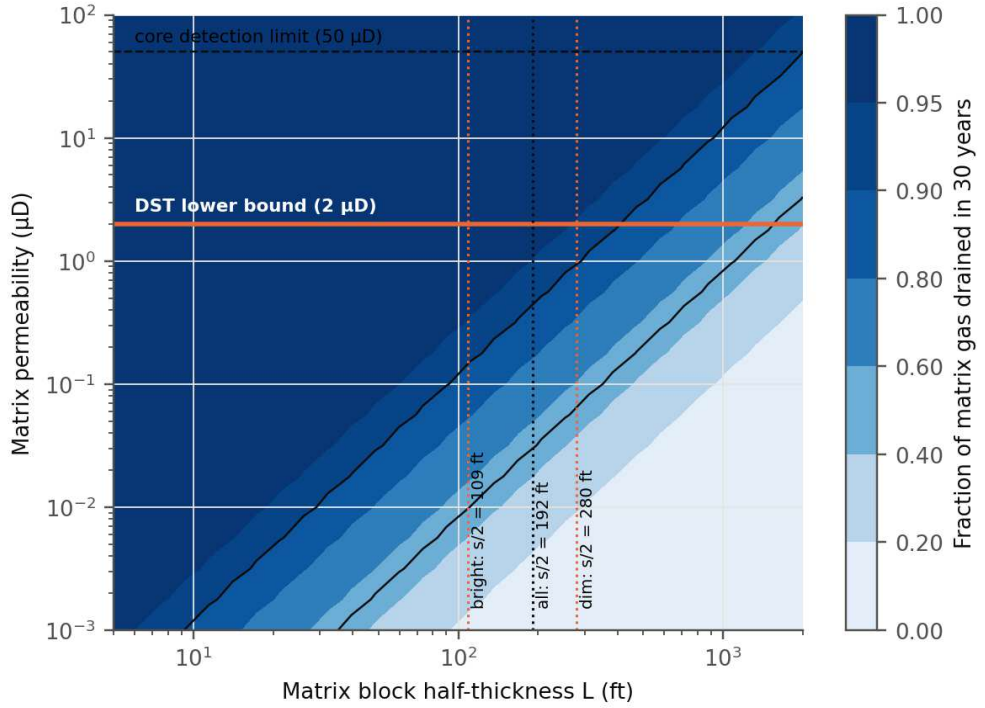


Fig. 5. Fraction of the gas in a matrix slab that drains to the bounding fractures in 30 years, as a function of matrix permeability and block half-thickness, for a fracture pressure falling linearly from 5,550 to 1,000 psia. Black lines: 50% and 90% contours. Orange line: the DST lower bound for the rock between flowing fractures. Dotted lines: half the conductive-fracture spacing (bright, field-wide and dim areas).

4.5 Field-scale recovery

The Monte Carlo estimate of gas initially in place is 5.3 Tcf (P10–P90 3.7–7.4 Tcf) (Table 3, Fig. 6b). With matrix permeability in the 2–50 µD bracket, 97% (92–99%) of the matrix gas is drained, and the technically drainable gas to 1,000 psia is 4.0 Tcf (2.8–5.7 Tcf), 78% of GIIP. If the DST lower bound were ten times too high, the drainable gas would be 3.7 Tcf (2.5–5.4); only in the pessimistic case of 0.01–0.1 µD would it fall to 1.6 Tcf (1.0–2.6). These figures are upper limits on recovery: they assume that every matrix block is bounded by fractures connected to a producing well and that the fractures do not fill with water.

Table 3. Field-scale results (Monte Carlo, 4,000 draws). E: fraction of matrix gas drained in 30 years. Drainable gas to 1,000 psia abandonment, before allowance for fracture connectivity and water. Values are P10 / P50 / P90.

Case	Matrix permeability	E	Drainable gas (Tcf)	Recovery factor (% GIIP)
GIIP	—	—	3.7 / 5.3 / 7.4	—
DST–core bracket	2–50 µD	0.92 / 0.97 / 0.99	2.8 / 4.0 / 5.7	73 / 78 / 79
DST bound ten times too high	0.2–50 µD	0.72 / 0.93 / 0.99	2.5 / 3.7 / 5.4	58 / 74 / 79

Case	Matrix permeability	E	Drainable gas (Tcf)	Recovery factor (% GIIP)
Pessimistic	0.01–0.1 µD	0.26 / 0.38 / 0.53	1.0 / 1.6 / 2.6	21 / 30 / 43

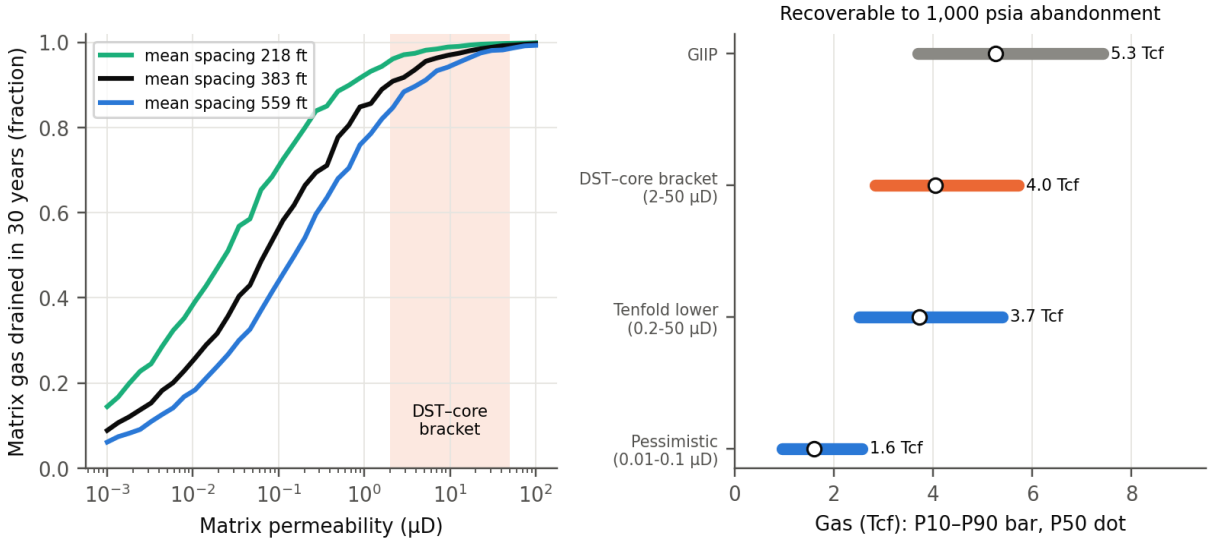


Fig. 6. (a) Fraction of matrix gas drained in 30 years against matrix permeability, for exponentially distributed block sizes with mean spacing 218 ft (bright top reflection), 383 ft (field-wide) and 559 ft (dim). Shaded: the DST–core bracket. (b) Gas initially in place and drainable gas to 1,000 psia for the three permeability cases (bars P10–P90, circles P50).

4.6 Mapping with the seismic

The conductive-fracture spacing differs between areas where the reflection from the Gargaf top is bright and where it is dim [9], so the seismic can carry the results of this study across the field. The positive-peak amplitude in the first 20 ms below the interpreted Gargaf top was extracted from the 3D SEG-Y volume, smoothed with a 300 × 300 m median filter (the window used at the wells) and divided at the well median (3,213), the threshold used to fit the spacings. The map reproduces the bright or dim class of 27 of the 28 wells inside the volume. It was combined with the depth map, the water level at −12,117 ft and the mid-case volumetric parameters (net-to-gross 0.775, porosity 0.035, water saturation 0.425) to map the gas in place, the drained fraction of the matrix and the chance that a well interval meets a flowing fracture (Fig. 7, Table 4).

Inside the seismic volume, 61 km² of Gargaf lies above the water level, about half bright (28.8 km²) and half dim (32.1 km²), with similar gas in place in each (about 1.7 Tcf). At the 2-µD lower bound the matrix drains 96% of its gas in bright areas and 84% in dim areas, so the drainable gas differs only modestly (1.28 against 1.15 Tcf). The difference grows if the matrix is tighter: at 0.2 µD the drained fractions fall to 80% and 55%. The larger contrast is in reaching the fractures. With flowing fractures about 220 ft apart, a 300-ft open interval has a 75% chance of meeting one in a bright area, but only 42% in a dim area; a 90% chance requires about 500 ft of open hole in bright areas and about 1,300 ft in dim areas. The gas-rich areas of Fig. 7b, high on the structure, are partly dim, so the gas that is easiest to produce and the gas that is easiest to reach do not coincide everywhere.

Table 4. Seismic-based comparison of bright and dim areas inside the SEG-Y volume, above the water level (mid-case volumetric parameters).

Quantity	Bright top reflection	Dim top reflection

Quantity	Bright top reflection	Dim top reflection
Area above water level (km²)	28.8	32.1
Mean conductive-fracture spacing (ft)	218	559
Gas initially in place (Tcf)	1.7	1.7
Matrix gas drained in 30 years, 2 µD / 0.2 µD	96% / 80%	84% / 55%
Drainable gas to 1,000 psia, 2 µD / 0.2 µD (Tcf)	1.28 / 1.07	1.15 / 0.74
Chance that a 300-ft interval meets a flowing fracture	75%	42%
Chance for a 1,000-ft interval	99%	83%
Open interval needed for a 90% chance (ft)	≈500	≈1,300

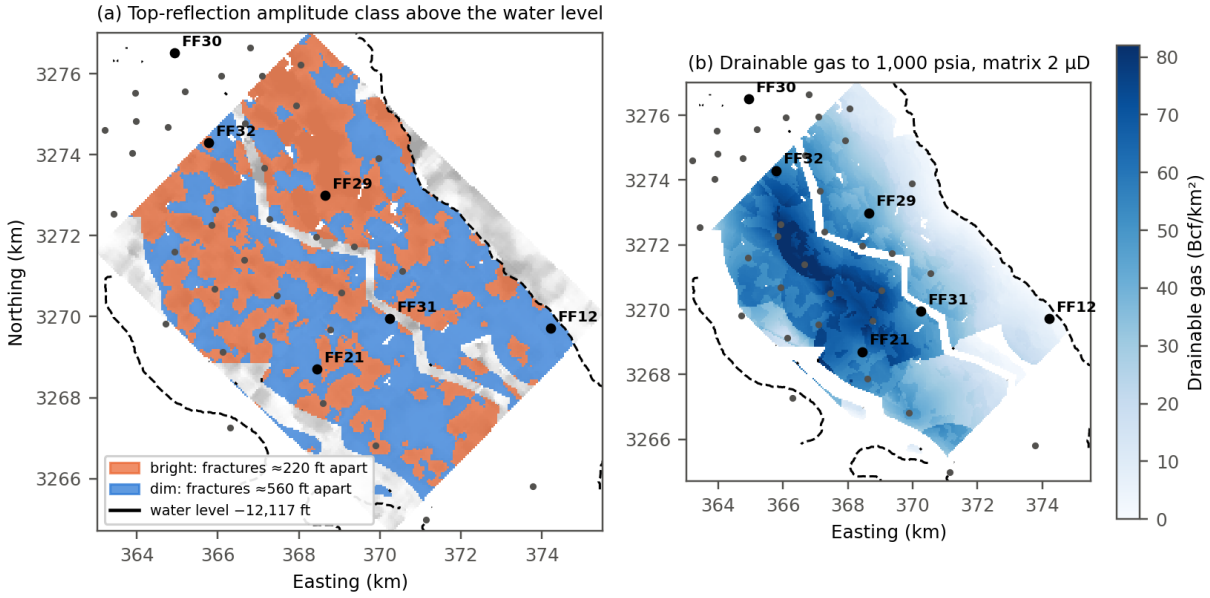


Fig. 7. (a) Areas where the reflection from the Gargaf top is bright (orange) or dim (blue) in the 3D seismic volume, above the water level at −12,117 ft (black line); grey: outside the gas column or no data; white strips: faults in the depth map. (b) Drainable gas per km² to 1,000 psia for a matrix permeability of 2 µD, from the gas column thickness, mid-case volumetric parameters and the drained fraction of each amplitude class. Large dots: wells with DSTs analysed in this study.

Figure 8 shows what the amplitude classes mean on the seismic. Along a section through FF32, FF29, FF31 and FF21, the Gargaf top is a continuous event, but the amplitude in the first 20 ms below it changes from bright to dim over a few hundred metres, giving the patchy pattern of Fig. 7a. FF29 and FF32 lie on bright patches, FF31 and FF21 on dim ones. Averaged over the wells, bright wells (13) show a strong trough about 20 ms above the picked top and a positive lobe within the first 20 ms below it; in dim wells (15) the trough above the top is weaker and the first 20 ms below the top contain a trough instead of a peak. The difference therefore lies in the shape and strength of the top-reflection complex, consistent with a change in the uppermost tens of metres of the quartzite [9].

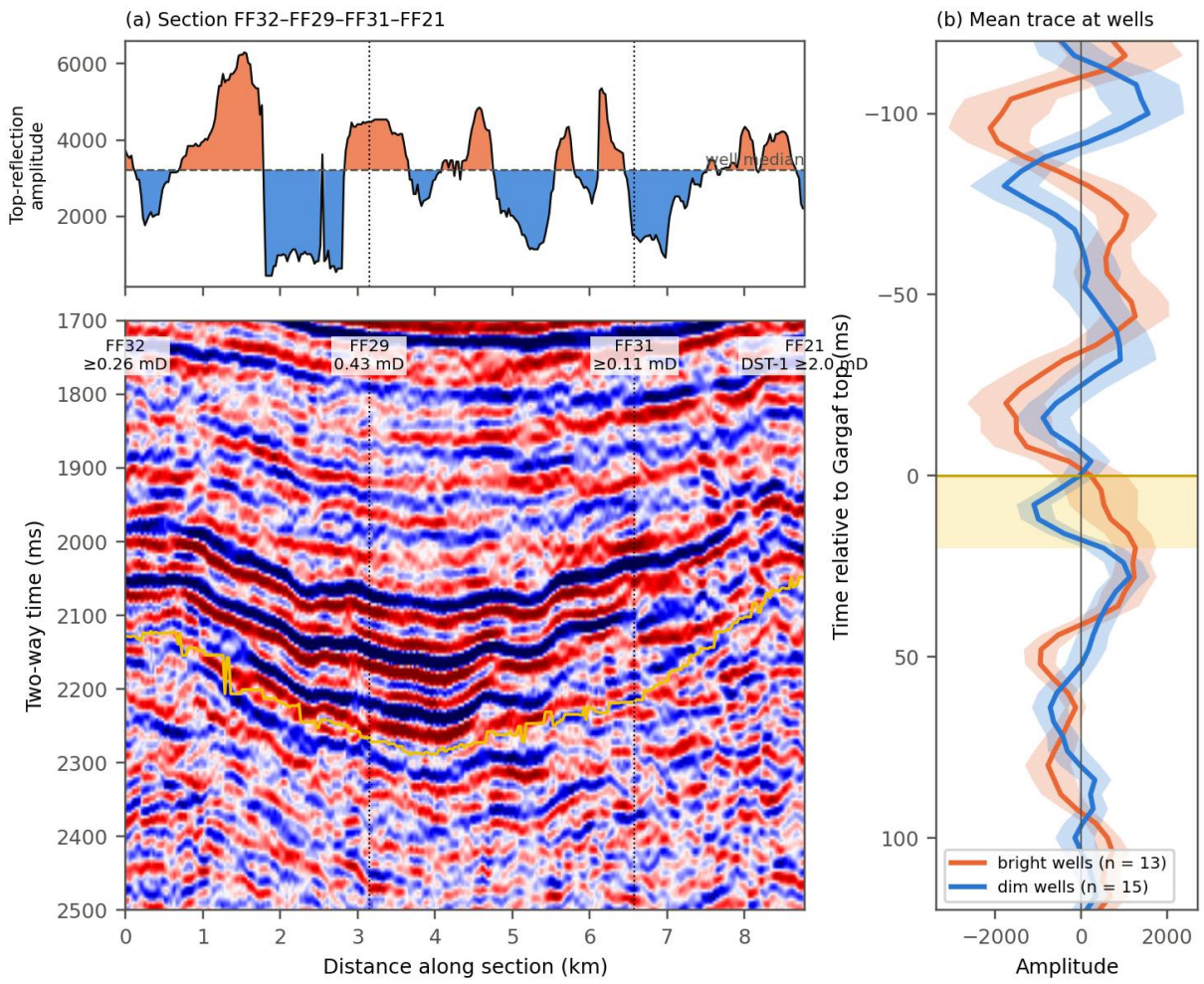


Fig. 8. (a) Section through wells FF32, FF29, FF31 and FF21 in the 3D seismic volume. Top: smoothed top-reflection amplitude (orange: bright, above the well median; blue: dim). Bottom: seismic amplitude (red–blue) with the interpreted Gargaf top (yellow); labels give the DST permeability from Table 2. (b) Mean seismic trace, aligned on the Gargaf top, at wells in bright (orange) and dim (blue) areas; shading: ± one standard error; yellow band: the 0–20 ms window.

Figure 9 turns the result into a simple guide for drilling. The chance that an open interval of length L meets at least one flowing fracture is $1 - \exp(-L/s)$. For a 300-ft interval it is 75% in bright and 42% in dim areas. To reach 90%, about 500 ft of open Gargaf is needed in bright areas but about 1,300 ft in dim areas, which is more than the gas column at many locations and therefore calls for deviated or horizontal wells there. Mapped on the structure (Fig. 9b), the crest between FF29 and FF32 is largely bright, while parts of the eastern flank and the area around FF21 and FF31 are dim.

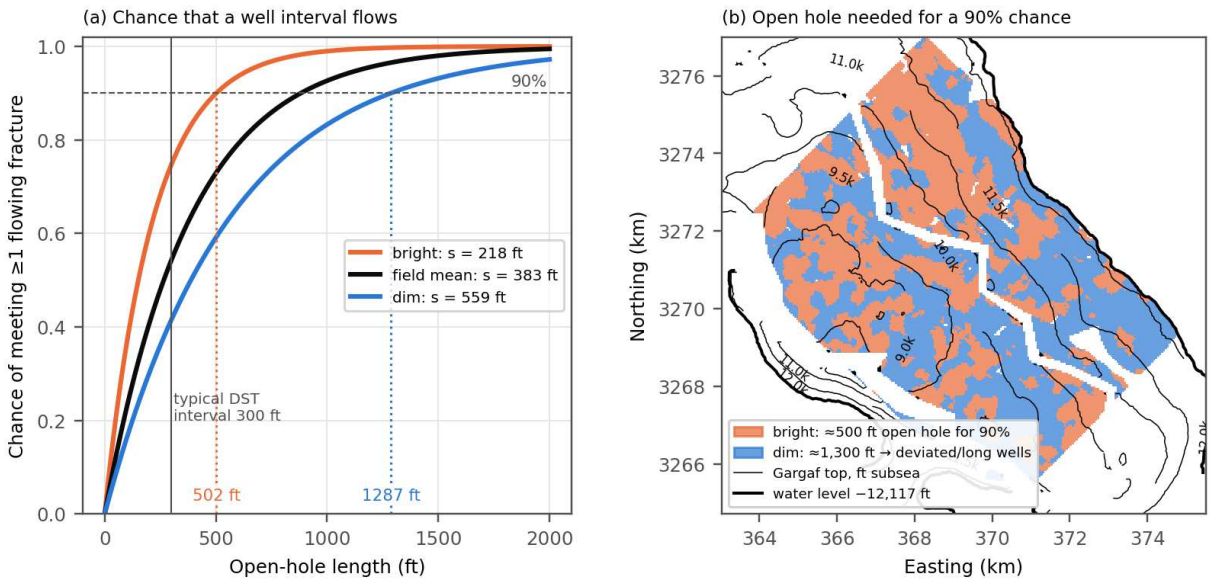


Fig. 9. (a) Chance that an open-hole interval meets at least one flowing fracture, against interval length, for the conductive-fracture spacing of bright areas (218 ft), the field mean (383 ft) and dim areas (559 ft). Dotted lines: length needed for a 90% chance. (b) Map of the open-hole length needed for a 90% chance (orange: about 500 ft; blue: about 1,300 ft), with Gargaf top depth contours (ft subsea) and the water level.

5. Discussion

5.1 Failed tests as measurements

Tight and low-rate DSTs are normally recorded as failures and set aside. This study shows that they constrain the quantity that core could not provide: the permeability of the rock between conductive fractures. In the Gargaf a single tight test places a lower bound of about 2 µD on it, and the core detection limit an upper bound near 50 µD. A lower bound is what the recovery question needs, because it is low matrix permeability that would strand gas. The approach requires only what most legacy well files contain, a pressure–time record of the shut-in and an estimate of the inflow, and it can be applied wherever routine core analysis has reached its floor. The FF21 tests show the main pitfall: a low-permeability result can reflect damage rather than tight rock, so tight DSTs give lower bounds, and intervals should be checked against earlier tests in the same well.

5.2 What limits recovery

At 2 µD or more the matrix is not a barrier. With the conductive-fracture spacing inferred in the same field, gas diffuses from the centre of a typical block to a fracture within one or two years, and at least about 90% of the matrix gas reaches the fractures within 30 years. A matrix three times tighter than the lower bound would still give up about 80% of its gas. The question “how much of the gas can be produced?” is therefore answered not by matrix permeability but by two other factors. The first is connectivity: only blocks bounded by fractures that are connected to a producing well are drained. About 40% of Gargaf DSTs are tight or weak [8], and in the dim-amplitude areas conductive fractures are more than twice as far apart as in bright areas [9]. The second is water. Formation water reaches the wells through the same fractures [8, 15], and where it fills the fractures around a matrix block it can trap gas in the block by imbibition. Development should therefore aim at connecting wells to the fracture network and at delaying water, rather than at stimulating the matrix.

5.3 Practical implications

Three practical points follow. First, because the matrix drains readily, the gas in place is a realistic target: in the bracketed case 78% of GIIP is drainable before connectivity and water losses, and the remaining risk lies in reaching it. Second, the derivative humps of the gas tests indicate positive skin, so the measured DST rates understate the deliverability of the same intervals; near-well treatments that restore or create a connection between the well and the fracture network, such as acidising fracture walls or short hydraulic fractures, are more promising than any matrix treatment. Third, test and completion intervals should be planned from the seismic map: about 500 ft of open hole gives a 90% chance of meeting a flowing fracture where the top reflection is bright, but about 1,300 ft is needed where it is dim, which favours deviated or horizontal wells in dim areas [8, 9].

5.4 Limitations

The lower bound on matrix permeability rests on one tight test (FF12 DST-2), whose inflow is estimated from the rise of the liquid column and whose radius of investigation is only a few feet; drilling-induced fractures could make it too high, although damage and effective-permeability effects would make it too low. Rates during DSTs are well-site estimates from wellhead pressure, and kh scales linearly with them; for FF31, FF32 and FF30 the rates were estimated here. Three gas tests give only lower bounds because the build-ups were too short. Interval-average permeability does not identify which part of the interval flows. The drainage model treats blocks as one-dimensional slabs, takes the spacing along the hole as the block thickness, uses a uniform fracture pressure and a single gas saturation, and ignores water and condensate; real blocks bounded in several directions drain faster, but water may trap gas. The GIIP inputs are those of the companion volumetric work and carry their own uncertainty. The seismic maps cover only the 3D sub-volume available (about 61 km² of the gas column), use two amplitude classes calibrated on 27 wells, and apply mid-case volumetric parameters everywhere. Finally, no production history was available, so the drainable gas is a prediction to be tested against production data, not a calibrated reserve.

6. Conclusions

1. Pressure records of nine legacy DSTs (1987–1997) in the Attahaddy Field were recovered from scanned well files and reinterpreted with pseudo-pressure and derivative analysis.
2. Gas and weak tests give interval-average permeabilities of 0.1–4.5 mD (three as lower bounds) after an early derivative hump from wellbore storage and positive skin; the DST rates therefore understate deliverability.
3. The tight Gargaf test FF12 DST-2 gives a lower bound of about 2 µD for the rock between flowing fractures; with the core detection limit this brackets it at about 2–50 µD. A low result in FF21 DST-2 reflects damage, showing that tight DSTs give lower bounds.
4. With the conductive-fracture spacing inferred from 60 Gargaf DSTs, at least about 90% of the matrix gas drains to the fractures within 30 years; the drained fraction would fall to 80% only below about 0.6 µD and to 50% below about 0.07 µD.
5. Of a gas initially in place of 5.3 Tcf (P10–P90 3.7–7.4), about 4.0 Tcf (2.8–5.7) is drainable to 1,000 psia; actual recovery is limited by fracture connectivity and water, not by the tight matrix.

6. Mapped with the 3D seismic, bright and dim areas hold similar gas, but a well needs about 500 ft of open hole in bright areas and about 1,300 ft in dim areas for a 90% chance of meeting a flowing fracture.

Declaration of competing interest

The author declares no known competing financial interests or personal relationships that could have appeared to influence the work reported in this paper.

References

1. Warren, J.E., Root, P.J., 1963. The behavior of naturally fractured reservoirs. Society of Petroleum Engineers Journal 3, 245–255.
2. Nelson, R.A., 2001. Geologic Analysis of Naturally Fractured Reservoirs, 2nd ed. Gulf Professional Publishing, Boston.
3. Aguilera, R., 1995. Naturally Fractured Reservoirs, 2nd ed. PennWell, Tulsa.
4. Kazemi, H., Merrill, L.S., Porterfield, K.L., Zeman, P.R., 1976. Numerical simulation of water–oil flow in naturally fractured reservoirs. Society of Petroleum Engineers Journal 16, 317–326.
5. Narr, W., 1996. Estimating average fracture spacing in subsurface rock. AAPG Bulletin 80, 1565–1586.
6. Hallett, D., 2002. Petroleum Geology of Libya. Elsevier, Amsterdam.
7. Hallett, D., Clark-Lowes, D., 2016. Petroleum Geology of Libya, 2nd ed. Elsevier, Amsterdam.
8. Alfakri, G., submitted. Fracture-borne water invisible to logs and core: evidence from drill-stem tests in a tight quartzite gas reservoir, Gargaf Formation, Sirte Basin, Libya.
9. Alfakri, G., submitted. The Gargaf top reflection predicts gas flow in a tight fractured quartzite where logs and core cannot: Attahaddy Field, Sirte Basin, Libya.
10. Horner, D.R., 1951. Pressure build-up in wells. Proceedings of the Third World Petroleum Congress, The Hague, Section II, 503–521.
11. Bourdet, D., 2002. Well Test Analysis: The Use of Advanced Interpretation Models. Elsevier, Amsterdam.
12. Tawadros, E., Rasul, S.M., Elzaroug, R., 2001. Petrography and palynology of quartzites in the Sirte Basin, central Libya. Journal of African Earth Sciences 32, 373–390. https://doi.org/10.1016/S0899-5362(01)90103-4
13. Sirte Oil Company, c. 2000. Integrated Reservoir Study, Bahi and Gargaf Intervals, Attahaddy Gas Field: Geology Interim Report III. Internal report, Marsa El Brega.
14. Alfakri, G., 2018. Integrated petroleum geosciences study of Attahaddy Gas Field (Sirte basin, Libya). 3rd World Congress on Petroleum Engineering and Natural Gas Recovery, Sydney. Journal of Petroleum & Environmental Biotechnology (conference abstract). https://doi.org/10.4172/2157-7463-C1-041
15. Alfakri, G., submitted. The gas–water contact of the Attahaddy Field is too deep: evidence from legacy logs, drill-stem tests, drilling records and pressures in a tight fractured quartzite reservoir (Gargaf Formation, Sirte Basin, Libya).
16. Sutton, R.P., 1985. Compressibility factors for high-molecular-weight reservoir gases. SPE Annual Technical Conference and Exhibition, Las Vegas, SPE 14265.
17. Hall, K.R., Yarborough, L., 1973. A new equation of state for Z-factor calculations. Oil and Gas Journal 71(25), 82–92.
18. Lee, A.L., Gonzalez, M.H., Eakin, B.E., 1966. The viscosity of natural gases. Journal of Petroleum Technology 18, 997–1000.
19. Al-Hussainy, R., Ramey, H.J., Crawford, P.B., 1966. The flow of real gases through porous media. Journal of Petroleum Technology 18, 624–636.
20. Bourdet, D., Ayoub, J.A., Pirard, Y.M., 1989. Use of pressure derivative in well-test interpretation. SPE Formation Evaluation 4, 293–302.

21. Agarwal, R.G., 1980. A new method to account for producing time effects when drawdown type curves are used to analyze pressure buildup and other test data. SPE Annual Technical Conference and Exhibition, Dallas, SPE 9289.
22. Lee, W.J., Wattenbarger, R.A., 1996. Gas Reservoir Engineering. SPE Textbook Series 5. Society of Petroleum Engineers, Richardson, TX.
23. Ramey, H.J., Agarwal, R.G., Martin, I., 1975. Analysis of "slug test" or DST flow period data. Journal of Canadian Petroleum Technology 14, 37–47.
24. Crank, J., 1975. The Mathematics of Diffusion, 2nd ed. Clarendon Press, Oxfo